Some Reservoir Engineering Calculations

for the Vapor-dominated System at Larderello, Italy

by

Manuel Nathenson

U.S. Geological Survey
Menlo Park, California 94025
April, 1975

U.S. Geological Survey
Open File Report 75-142

Some Reservoir Engineering Calculations for the Vapor-dominated System at Larderello, Italy

by Manuel Nathenson

U.S. Geological Survey

Menlo Park, Califoria 94025

Abstract.--Various reservoir properties are calculated for the Larderello vapor-dominated system using available published data. Bottom-hole flowing properties are calculated from measured wellhead data. Whereas wellhead temperatures measured at a particular time tend to change systematically with changes in flow and pressure, calculated bottom-hole temperatures tend to be constant for two sample wells; while for a third, bottom-hole temperatures decrease with increasing flow. Bottom-hole temperatures calculated from wellhead data taken over several years can be constant, increase, or decrease for particular wells. A steady-state model for steam flow to a well is used with calculated bottom-hole data to show that the effect of non-Darcy flow is important. The initial mass of fluid in place for the northeast zone of Larderello (56 km^2) is estimated, using data on shut-in pressures and total mass production. Reservoir thickness needed to store this mass of fluid is calculated as a function of porosity and initial fraction of water in pores. Representative values are 19 km of thickness, assuming 5% porosity with steam alone, and 832 m, assuming 20% porosity and 10% of pore volume as liquid water.

Introduction

The purpose is to present some reservoir engineering calculations for the vapor-dominated system at Larderello, Italy using available published data. The published data are inadequate for a thorough understanding of the reservoir; however, several important points concerning the response to production can be made. The various models for the production of steam from vapor-dominated reservoirs have been recently reviewed and extended by Truesdell and White (in press) and will not be discussed here. My purpose is to provide some quantitative results to aid in understanding the reservoir.

The first section concerns bottom-hole properties of flowing steam wells calculated from measured wellhead data. The reason for this calculation is that the temperature of the fluid at bottom of the hole is characteristic of the formation and is needed to understand the reservoir, while its value at the wellhead includes large effects from flow up the well. Calculations are made for both flow rate versus wellhead pressure data and flow-time data. The next section is a simple steady-state model for steam flow in the formation to a well. This is used with flow rate versus bottom-hole pressure values (calculated from measured wellhead data) to estimate permeability-thickness product. Using correlations for non-Darcy flow, order of magnitude estimates of thickness and permeability are also made. The last section uses the limited amount of shut-in pressure data and total mass of produced fluid to estimate the initial mass of fluids in place for the northeast zone of Larderello. Using an assumed value for reservoir area, the initial mass of fluid in place permits discussion of reservoir thickness as a function of volume fraction of liquid in pores and porosity.

Bottom-Hole Flowing Properties

Theory

Previous calculations for bottom-hole flowing pressure made by Rumi (1967, 1970, 1972) did not attempt to include the effects of heat transfer. The present formulation is approximate but includes the major elements of heat transfer and the thermodynamic properties of steam as a non-ideal gas.

The physical situation involves steam flowing at a mass rate M in the formation in a zone of vertical thickness L at a velocity that can be considered negligable as long as $L >> r_w$, where r_w is the wellbore radius. Just before entering the well, the steam is at a state denoted by the subscript BH (for bottom-hole) of pressure P_{BH}, enthalpy h_{BH}, temperature T_{BH}, and specific volume V_{BH}. The steam then flows up the well losing pressure due to friction, gravity, and increasing momentum and losing enthalpy from conductive heat transfer to surrounding cooler rocks. The steam exits at the wellhead with properties denoted by the subscript WH.

Defining the mass velocity as G = u/V where u is the flow velocity and V is the specific volume, we can write conservation of mass, momentum, and energy as:

$$M = G\,\pi r_w^2 = \text{const.} \tag{1}$$

$$\frac{dP}{dz} + G^2\frac{dV}{dz} = -\frac{g}{V} - \frac{\lambda G^2}{4r_w}V \tag{2}$$

$$M\frac{d}{dz}\left[h + \frac{1}{2}G^2V^2 + gz\right] = \frac{-dq}{dz} \tag{3}$$

where λ is the friction factor for pipe flow, g is the acceleration of gravity, z is length along the well from the point of steam entry, and

$\frac{dq}{dz}$ is the heat lost to the formation per unit length. To calculate the heat transferred to the wall rock, the formulation of Ramey (1962) is used. The set of equations is completed by adding the thermodynamic properties of steam of specific volume and enthalpy as a function of temperature and pressure, i.e. $V = V(P,T)$ and $h = h(T,P)$. The set of equations (1) to (3) is difficult to solve exactly, because the thermodynamic properties of steam cannot easily be expressed as analytical functions and the property relations depend on both temperature and pressure.

Because of the characteristics of flowing steam wells, simple approximations can be developed that retain the main functional dependence of the thermodynamic properties of steam, yet allow equations (1) to (3) to be solved without a large computer. Since the pressure decreases up the well from about one half to a few bars and the temperature from a few degrees to a few tens of degrees, the equation of state $V = V(P,T)$ can be approximated for purposes of calculating pressure drop as

$$PV = P_{WH}V_{WH} \tag{4}$$

where P_{WH} is known and V_{WH} is obtained from the steam tables (Keenan and others, 1969) for the known values of P_{WH} and T_{WH}. When the flows are low and temperature changes in the well are great, this approximation is less satisfactory; however, then the pressure drop in the well is small, and the inaccuracy is not very important. This approximation will be further checked in some of the calculations.

One more approximation is required to integrate equation (2). We can rewrite equation (2) in the form

$$\frac{1}{V}\frac{dP}{dz} + G^2\frac{d\ln V}{dz} = \frac{-g}{V^2} - \frac{\lambda G^2}{4r_w},$$

and then substitute equation (4) in the first term to obtain

$$\int_{P_{BH}}^{P_{WH}} \frac{dP^2}{2P_{WH}V_{WH}} + \int_{V_{BH}}^{V_{WH}} G^2 d(\ln V) = -\int_0^H \left(\frac{g}{V^2} + \frac{\lambda G^2}{4r_w}\right) dz. \qquad (5)$$

One way to integrate this equation is to neglect the term $G^2 d\ln V$, but at low wellhead pressures and high flows, this term is significant so it should be kept. The second way is to realize that when pressure changes are large, they are caused by the last term in equation (5) due to high mass flows. When the gravity term g/V^2 dominates, pressure drops are not large. Equation (5) may then be integrated by approximating the integral of g/V^2 over the flow length H. Assuming a linear distribution of density $1/V = 1/V_{BH} + (1/V_{WH} - 1/V_{BH})(z/H)$, we can integrate the term g/V^2 approximately and the rest of the terms exactly. Substituting equation (4), we obtain

$$\frac{P_{BH}^2 - P_{WH}^2}{2P_{WH}V_{WH}} = \frac{\lambda G^2 H}{4r_w} + \frac{gH}{3V_{WH}^2}\left[\left(\frac{P_{BH}}{P_{WH}}\right)^2 + \frac{P_{BH}}{P_{WH}} + 1\right] + G^2 \ln\frac{P_{BH}}{P_{WH}}. \qquad (6)$$

The unknwown P_{BH} appears on both sides of equation (6). Since the ratio P_{BH}/P_{WH} is usually near one and at most 2 or 3, equation (6) can easily be solved by substituting a guessed value of P_{BH}/P_{WH} into the right-hand-side, solving for P_{BH}, resubstituting P_{BH}/P_{WH}, and finding a new P_{BH}. Normally two iterations are sufficient to obtain agreeement to 0.05 bar. This type of operation is ideally suited for solution by using a small programmable calculator, and this has been done.

The equation of energy conservation (3) may be formally integrated to

$$h_{BH} = h_{WH} + \frac{1}{2} G_{WH}^2 V_{WH}^2 + gH + \frac{q}{M} \qquad (7)$$

where the kinetic energy of the steam entering at the wellbore radius has been neglected. The heat transfer q actually depends on the detailed temperature distributions in the wall rock far from the well and in the bore itself. The former is unknown for all of the field data to be used here. A reasonable approximation is to assume that the rock temperature far from the well follows a conductive gradient from the mean annual temperature at the surface to the reservoir temperature at the top of reservoir at a depth H_T. Studies at Larderello (Burgassi and others, 1961; Boldizsar, 1963) show that the measured heat flow far removed from flowing wells is either that value or within a factor of two of that value. White and others (1971) measured heat flows orders of magnitude higher in regions very near to fumaroles and mud pots of the natural vent areas of the Mud Volcano system of Yellowstone Park, Wyoming, but production wells are not normally drilled in an active vent area. The temperature distribution in the well is near enough to isothermal that the overall heat transfer can be calculated by assuming a constant temperature in the wellbore.

The rate of heat conduction from the well to the rock may be written as

$$\frac{dq}{dz} = \frac{2\pi \, k_{TH}(T - T_e)}{f(t)} \qquad (8)$$

where k_{TH} is the thermal conductivity, T is the well temperature, T_e is the earth temperature both at coordinate z and f(t) is a function of time obtained from the solution for a cylindrical source of radius r_w at

constant temperature (Ramey, 1962). Equation (8) is only valid at time long enough for the temperature in the well to be approximately steady, i.e. after several wellbore volumes have come out of the well. Substituting the assumed temperature distributions and integrating from 0 to H, we obtain

$$q = \pi k_{TH}(T_{BH} - T_{eo})H/f(t) \qquad (9)$$

where T_{eo} is the temperature of the ground at the surface. If the data were more complete, it is likely that the depth to uniform reservoir temperature H_T would be different than the depth to steam entry H. Since I have no such data, I have set $H_T = H$ in Eq. (9).

The procedure for using equations (6), (7) and (9) to obtain bottom-hole flowing conditions is as follows. For equation (6), the quantities H and r_w are known, P_{WH} is measured, G is calculated from equation (1), and V_{WH} is obtained from the steam tables for the measured values of P_{WH} and T_{WH}. The friction factor λ can be obtained from Katz and others (1959) for values of surface roughness and Reynolds number ($2M/\mu r_w$). For typical outputs of Larderello wells (above 5 kg/sec) in a well of 32 cm diameter and 0.0015 cm = 0.0006 in. surface roughness, the Reynolds number is high enough that the flow is fully turbulent, and the friction factor is approximately constant at a value of 0.011. For low flows, the friction factor is larger but the pressure drops become small enough that the variation in friction factor is not significant. Equation (6) may now be solved by iteration for the value of P_{BH}.

The bottom-hole enthalpy is calculated from equation (7). Values for h_{WH} and V_{WH} are obtained from the steam tables for the known well-head conditions. The heat transfer term is calculated from equation (9). The value of the function f(t) is obtained from Ramey (1962).

After flow times on the order of a few weeks needed to heat rocks near the well, the function f(t) changes slowly with time. Actual thermal conductivities are not known for the various wells, but the data of Boldizsar (1963) indicate that 3 mcal/cm sec °C is fairly representative. The volumetric specific heat of earth materials is nearly constant at 0.6 cal/cm^3°C (Lachenbruch as quoted in White, 1965). These values together with the well radius (16 cm for a typical Larderello well) are used to obtain the dimensionless time and then the value of f(t). At one year f(t) is 3.8, while at 5 years it is 4.6; therefore, it is not a strongly varying function. The use of standard thermal conductivity in equation (9) is a bit more suspect as the heat transfer is a linear function of k_{TH}, but there is no alternative as adequate data for the specific wells are not available. Substituting the heat transfer value from Eq. (9) into (7), we obtain a value for the bottom-hole enthalpy. Using this value and the calculated bottom-hole pressure, the bottom hole flowing temperature is obtained from the steam tables.

Examples and discussion

An index map of the wells to be considered (figure 1) is adapted from Sestini (1970). Relevent physical data are given in table 1. In order to show some workings of the calculations, the answers for well VC 10 are presented in greater detail than for the others. Well VC 10 has a total depth of 1088 m, with fissures at 950 and 1030 m; there is 826 m of "impervious cap rock" above the crystalline basement (Sestini, 1970, p. 634) with no Triassic evaporite formation appearing. For calculating bottom-hole flowing conditions, Rumi (1970, p. 699) used a 796 m depth to steam which I will also use, and he gives the diameter as 32 cm. The wellhead characteristics in 1963 are given by Sestini (1970, p. 641), and flow time data are given in his Figure 8. The parameters for heat transfer calculations used in equation (9) are 3 mcal/cm sec°C conductivity, 250°C temperature difference, and one year flow time prior to the measurements in 1963. The pressure and temperature distribution along the length of the bore can be calculated from slightly different forms of equations (6), (7) and (9), with the modifications being an extra kinetic energy term in (7) and the variation of heat loss with depth. Figure 2 shows the distribution of flowing temperatures and pressures in VC 10 for a flow of 37.5 kg/sec and wellhead pressure of 5 bar and temperature of 244°C. Notice that there are quite large compressibility effects, but the assumption used to calculate the small gravity-term in equation (5) of linearly decreasing density up the well should be quite good, since the pressure is nearly linear. The short horizontal line at 796 m in the temperature diagram shows the change in temperature from accelerating the flow from a low velocity in the formation to its higher

value in the bottom of the well. Figure 3 shows the well characteristics of VC 10. The measured data are mass flow and wellhead (WH) temperature as a function of wellhead pressure; the bottom-hole (BH) values are calculated. The bottom figure shows the mass flow as a function of wellhead and bottom-hole flowing pressures. The top figure shows wellhead and bottom-hole enthalpies. It is important to note that the bottom-hole properties shown in the top two figures are plotted as a function of bottom-hole pressures. A set of wellhead and bottom-hole points are connected by a broken line to show this correspondence.

In calculating enthalpies and temperatures, there is an ambiguity when Mach number effects become important. At low wellhead pressures and high flows, the steam velocity in the upper part of the well approaches the speed of sound; sometimes the flow actually attains sonic velocity at the exit. Above a Mach number (flow speed/local sound speed) of about one third, increasingly significant amounts of internal energy are converted to kinetic energy. In measuring the temperature under conditions of high velocity flow, a probe will measure something between the temperature of flowing steam, called the static value, and the temperature of the flow after it has been brought to rest by a reversible adiabatic process, called the total temperature; see, e.g., Liepmann and Roshko (1957). Judging from figure 5 of Nencetti (1964), the flowing temperature measurements seem to have been taken without any special precautions, so the measured temperatures are somewhere between total and static values. The enthalpy values shown in the top figure are obtained from the steam tables by assuming that the measured temperatures were static values. The middle figure shows measured wellhead

temperatures. Two bottom-hole temperatures have been calculated by assuming that 1) wellhead temperatures are static values (BH-S) and 2) wellhead temperatures are total values (BH-T). Clearly there is significant uncertainty in calculating flowing bottom-hole temperatures because of the uncertainty in significance of the measured wellhead temperatures.

The purpose of presenting the temperatures and enthalpies for a flowing well is to use them to understand better the nature of the reservoir and the mechanics of fluid production. It is clear from figure 3 that most of the temperature variation measured at the wellhead is produced by flow and heat transfer that take place in the well and have little to do with reservoir processes. Considering the accuracy of the data and the uncertainties in the calculations, the bottom-hole flowing temperature is concluded to have been nearly constant for the length of time needed to measure the wellhead characteristics of VC 10. The significance of this to reservoir mechanics is discussed below. The calculated bottom-hole temperature at the highest bottom-hole pressure (29.4 bar) is lower than the value at 17.8 and 22.3 bar, and it is not clear if this represents an uncertainty or a real effect. In order to produce a flow with nearly constant bottom-hole temperatures, the formation must produce steam whose enthalpy increases as bottom-hole flowing pressure decreases (top of figure 3).

Another well for which fairly complete data are available is Gabbro 9. From Rumi (1970, p. 700), the depth to the steam zone is about 859 meters and the well diameter is 32 cm; Pollastri (1970, p. 783) gives the wellhead characteristics. Heat transfer parameters for equation (9)

are 3 mcal/ cm sec°C conductivity, a 230°C difference between the earth surface and reservoir temperatures far from the well, and production for one year prior to the measurements. The measured wellhead and calculated bottom-hole flowing conditions are shown in figure 4. Bottom-hole temperatures calculated by assuming that wellhead temperatures are static are again marked BH-S, and total temperatures are marked BH-T. The differences in calculated values are larger than for VC 10 because the lowest wellhead pressure here is 2.9 bar. The shapes of the flowing temperature curves are similar to those for VC 10, but they are uniformly lower. Gabbro 9's wellhead temperatures are representative of the Larderello area as there are very few wells with temperatures as high as in VC 10. The calculated bottom-hole temperatures for Gabbro 9 also seem to be fairly constant. At low flow and high pressure, they show the same dip as those for VC 10.

The previous two wells are examples of more productive wells. An example of a poor quality well is St. Silvestro (Sasso Pisano) whose measured wellhead characteristics are shown in figure 5 (Pollastri, 1970) with an expanded mass-flow scale compared to previous figures. With a similar shut-in pressure to Gabbro 9 of about 20 bars, the St. Silvestro well has only about 1/6 the flow of Gabbro 9 and therefore has a much lower permeability or is damaged. In wells with low rates of flow, wellbore heat losses are sufficient to convert dry steam to slightly wet steam. In figure 5, the measured wellhead temperatures at low pressure and high flow are joined by a straight line. At the higher pressures and lower flows, the data points follow the saturation pressure-temperature curve (Keenan and others, 1969) shown as a broken line. No

physical dimensions are published for this well, but we assume representative values of 700 m depth to steam and a 32 cm diameter. Assuming production for one year prior to the measurements, the flowing bottom-hole pressure and temperature can be calculated and are shown in figure 5. Because of the low flows, pressures change very little in the well, and the curves for WH and BH nearly coincide. For the wellhead data point at 11.7 bars (just on the saturation line), steam is assumed to be just saturated, with no liquid water. At higher pressure and lower flows the wellhead fluid has an unknown fraction of liquid water so its bottom-hole state cannot be calculated from the available data. The important point of these few bottom-hole temperatures is that they clearly increase with bottom-hole pressure, unlike the previous calculations. The physical process at the well bottom seems to be basically different from the previous wells. The reason for this is probably related to the location of this well in an area where there are quite a few "dry" (non-producing) wells (Marchesini and others, figure 4, 1962) which may indicate an edge zone of a steam reservoir.

Flow-time data

A subject of some importance to the exploitation of the Larderello field is the variation of flows, temperatures, and gas contents of individual wells with time (see, e.g. Sestini, 1970 and Truesdell and White, in press). The purpose of this section is to use the calculation procedure to change measured wellhead properties to bottom-hole properties. This is a useful step in trying to get at the thermodynamic path of the exploitation but gives little insight into the variations in flows or gas contents with time.

The application of the above calculation procedure would be straightforward, except for the scarcity of wells for which dimensions and production histories are available. In order to get around this problem, these calculations are based on a hypothetical standard well assumed to be 32 cm (12.6 in.) in diameter, 700 m (2297 ft) deep, and with a friction factor of 0.011; the formation has thermal conductivity of 3 mcal/cm sec°C, the well has been producing for one year, and the temperature difference for equation (9) is 210°C. This choice of parameters results in a conductive heat transfer, from equation (9), of 153 k J/sec. For longer producing times or different bottom-hole temperatures, this number would change, but the use of assumed constants introduces enough uncertainty for this variation to be neglected.

Results for pressure decrease from bottom-hole to wellhead conditions are shown in figure 6. The top figure is for wellhead pressure of 5 bar and the bottom figure for 6 bar. In each figure, a curve is shown for wellhead temperatures of 170 and 240°C. This change with wellhead temperature reflects the influence of the specific volume in equation

(6). For a given flow rate near production conditions, figure 6 shows the pressure drop to be about as sensitive to a 1 bar change in wellhead pressure as to a 70°C change in flowing temperature. Larderello wells generally have flows at producing pressures from 50 to 100 x 10^3 kg/hr, so their pressure drops are on the order of 1-1/2 to 4 bar.

Results for the enthalpy decrease from bottom-hole to wellhead are shown in figure 7. The top figure is for 5 bar wellhead pressure and the bottom figure is for 6 bar. The q term in equation (7) is the same for both temperatures shown in each figure. The differences in enthalpy change caused by wellhead temperature change are from the kinetic energy term in equation (7). The solid curves in figure 7 are obtained assuming that wellhead temperatures are static temperatures. The broken curve shows the change in total enthalpy up the well, and it is obtained from the terms gH + q/M. The differences between the broken and solid curves are due to the kinetic energy at the wellhead $(G_{WH}V_{WH})^2/2$, since the bottom-hole kinetic energy is assumed negligible. At low flows, figure 7 shows that wellbore heat loss dominates, while at high flows the kinetic energy is a fairly large term. For normal flows of 50 to 100 x 10^3 kg/hr, the decrease in enthalpy from bottom-hole to wellhead is a fairly weak function of mass flow. Within this range of flows, differences in wellhead temperatures from well to well are a good indicator of differences in bottom-hole properties. At flows either above or below this range, it is quite dangerous to make comparisons using wellhead properties, and one must use bottom-hole properties. Of course, in the range of high flows the uncertainty in wellhead temperatures due to kinetic energy effects becomes large.

Before applying these standard well curves, the limited data for VC 10 will be discussed. The dimensions of this well are known, but production data have been published for only a few years of its life (Sestini, 1970, p. 634). For 1966 through part of 1969, calculations using the constants given earlier and with two years of production prior to 1966 (Sestini, 1970, figure 8) show that the temperature drop up the well is nearly constant at 13°C if the measured wellhead temperature is taken as the static temperature. For this period, the wellhead temperature is approximately constant, thus the bottom-hole temperature is also approximately constant at about 271 or 273°C, which agrees with the calculated values in figure 3. Sestini (1970) provides temperature and flow data for 1964 and 1965, but the wellhead pressure, which was clearly much higher in this early period, is not plotted.

Figures 8, 9 and 10 show measured wellhead and calculated bottom-hole properties using the standard-well curves for three wells whose locations are shown on Figure 1. The data for Prata 2 and 4 are from Sestini (1970, p. 634) and for Larderello 85 are from Ferrara and others (1970, p. 579). For Prata 4, the flows are low enough that the effect of Mach number is negligable. For Prata 2, the difference between assuming total or static wellhead temperatures is several degrees and constant, so only calculations assuming static temperatures are shown. For Larderello 85, the flows are much larger and quite variable, ranging from 255 to 70 x 10^3 kg/hr, so calculated bottom-hole temperatures are shown, assuming either static or total wellhead temperature was measured. The three sets of data show the wide range of possible temperature patterns. Prata 2 has essentially constant wellhead and bottom-hole temperatures,

in contrast to Prata 4 which has continually rising wellhead and bottom-hole temperatures. Larderello 85 has rising wellhead temperatures but declining bottom-hole temperatures.

The set of data for Prata 2 and 4, which are about 700 m apart, go together to form a very interesting picture. Nencetti (1964, p. 33) reports shut-in pressure histories in these wells. The data were presented in 1961 suggesting that they were obtained in the early part of exploitation of the Prata zone. Prata 2 stabilized to a shut-in pressure of 31.6 bar in less than 50 hours. Adding a reasonable weight of steam column, the shut-in pressure at the bottom of the hole was about 31.8 bar which corresponds to a temperature of saturated steam of 237°C. This 237°C temperature is in good agreement with the calculated bottom-hole temperature in figure 8, and the agreement indicates that the well taps a region which was initially filled with saturated steam and now has since been produced isothermally due to the stored energy in the rock. Prata 4 stabilized to 30.6 bars after a period of nearly 500 hours or ten times that of Prata 2's stabilization period. Adding a reasonable weight of steam column, the bottom-hole shut-in pressure of Prata 4 is about 30.8 bars which corresponds to a temperature of saturated steam of 235°C. The highest calculated bottom-hole temperature in figure 9 for Prata 4 is 214°C. This behavior cannot be explained by a well tapping a reservoir of only steam, and indicates liquid water close to the bore. The quantity of flow in this well implies a reasonable value of permeability, so the behavior cannot be explained by a single liquid-filled zone of low permeability producing itself to dry steam. Without more data on the temperature distribution with depth of the

inflowing steam, the effects of a shallow casing, which may allow near surface liquid water to mix with steam from the reservoir, cannot be separated from the effects of a steam zone with dispersed pore water boiling to steam.

The pressure recovery data given above has been analyzed by Elder (1965, 1966). His interpretation was that the slow recovery of Prata 4 reflected a low permeability for the well, a factor of 100 less than that for Prata 2, but he lacked flow and temperature data. Because the flows of the two wells are within a factor of two, the permeabilities should be within a factor of two. The explanation for their different pressure recoveries then is that the boiling process involved in Prata 4 probably creates a dried volume around the well (Truesdell and White, in press). When the well is shut-in, pressure and temperature gradients exist from zones with liquid water still available to the dried volume. Steam flows towards the well to even out the pressure distribution, but the nonuniform temperatures cause it to condense in the dried volume. Pressure gradients will continue to exist until enough mass transport takes place so that no part is out of equilibrium with respect to the saturation curve. This is a much slower process than the simple pressure recovery of Prata 2.

The data and calculations for Larderello 85 (figure 10) also illustrate an important point. The measured wellhead temperatures increased continually over the ten year period. The large decrease in bottom-hole pressure as the flow declines changes this into a decline in the bottom-hole temperature. The large and rapidly changing flow of this well is not representative, but it illustrates clearly the danger of interpretations based only on wellhead temperatures.

RESERVOIR CALCULATIONS

Flow to a well

In an earlier section, wellhead data were used to calculate mass flow as a function of bottom-hole flowing pressure. The next logical step is to use flow in porous media to analyze this bottom-hole behavior. One can conceive of many models of liquid-vapor distribution in the reservoir, but this calculation assumes that the flow is entirely steam. From the quantity of fluids that have been produced at Larderello, most of the steam must come from the boiling of liquid water (see discussion below); however, the contour maps for the central zone of Larderello of shut-in pressure presented by Ferrara and others (1970) show an average decline in pressure on the order of 6 bars between 1959 and 1969, so a significant part of the steam production is related to the declining steam pressure. Anticipating the results, the analysis shows that large effects result from what is called "turbulent" flow in porous media. The physical cause of this extra resistance is most likely inertia effects rather than turbulence (e.g., see Gewers and Nichol, 1969), but the terminology of calling it turbulent flow is already well established. The treatment which follows is similar to Katz and others (1959).

Assuming steady radial flow of mass rate M to a well through a thickness L, the governing equations are

$$\frac{qr}{V} = \frac{M}{2\pi L} = \text{const.} \tag{10}$$

$$\frac{dP}{dr} = \frac{\mu}{k} q + \beta \frac{q^2}{V} \tag{11}$$

$$PV = \text{const.} \tag{12}$$

where q is the specific discharge, V is the specific volume, μ is the viscosity, k is the permeability, and β is the turbulence coefficient (see for example Katz and Coats, 1968). From the earlier calculations, the bottom-hole temperature for some wells is reasonably constant, so equation (12) should be a reasonable representation of the thermodynamic path. Combining equations (10) and (11) and integrating from the well-bore where $P = P_{BH}$ at $r = r_w$ to the drainage radius r_e where $P = P_o$, (P_o is the shut-in pressure at the time the test is being run), we obtain

$$\int_{P_{BH}}^{P_o} \frac{dP}{V} = \frac{\mu M}{kL2\pi} \ln \frac{r_e}{r_w} + \frac{\beta M^2}{4\pi^2 L^2} \left(\frac{1}{r_w} - \frac{1}{r_e} \right) . \qquad (13)$$

Note that the thermodynamic path enters only through the integral on the left hand side of equation (13). Substituting equation (12) and performing the integration, we obtain

$$\frac{P_o^2 - P_{BH}^2}{2P_o V_o} = \frac{\mu M}{kL2\pi} \ln \frac{r_e}{r_w} + \frac{\beta M^2}{4\pi^2 L^2} \left(\frac{1}{r_w} - \frac{1}{r_e} \right). \qquad (14)$$

When using equation (14) the value of V_o is obtained from the steam tables from the known value of bottom-hole shut-in pressure P_o and the calculated bottom-hole flowing temperature.

In order to see the need for the turbulence term to satisfy the data, figure 11 shows the calculated bottom-hole conditions for VC 10 from figure 3 replotted in two ways. The top figure shows mass flow versus bottom hole pressure squared and the bottom figure shows the mass flow versus the difference of the square of the pressures divided by the mass flow. If the last term in equation (14) were negligible, the data in the upper plot would be on a straight line, which it clearly is not.

Part of the nonlinearity shown in the top figure is actually caused by the use of equation (12). As the value of pressure difference $P_o - P_{BH}$ increases, the use of equation (12) causes an error which also increases. Assuming the flow to be isothermal, the integral in equation (13) has been evaluated numerically by using steam table data. Over the range of pressures, the error increases from 0 to a maximum of 3%, and this error is not large enough to account for the shape of the curve. The bottom plot in figure 11 provides a quantitative measure of the importance of the second term in equation 13. For pure Darcian flow (β=0), data plotted in these coordinates would be a vertical line. For pure turbulent flow, data would plot as a line through the origin. The data for VC 10 is somewhere in between these two limits.

As the bottom plot in figure 11 shows, the data seem to have a functional form consistant with equation 14. This consistancy may be checked further by combining these results with one of the correlations of turbulence factor with permeability. Probably no single relation exists between permeability and turbulence factor that is valid for all reservoir materials, and data are lacking for Larderello. For example, the correlation of Gewers and Nichol (1969) for microvugular carbonates may be written as $\beta = 1.6 \times 10^{10}/k^{1.41}$ where k is in mdarcy and β in cm^{-1}. Taking the intercept and a point on the line from the bottom part of figure 11, we can use equation 14 with $r_e/r_w = 500$ to calculate the permeability-thickness kL as 99 darcy-m and, with the correlation, the permeability as 15.8 darcy and the thickness L as 6.2 m. If we use the Katz and Coats (1968) correlation for sandstone, which is probably less valid for the rocks at Larderello, we obtain k = 320 darcy and L = 0.3

m. Clearly with no data on the Larderello reservoir material, these numbers can be no more than order-of-magnitude, but they are illuminating. Both sets of calculations imply that the flow to the well is in a relatively thin region of the order of meters thick and high in permeability. Counter to this, the calculations of reservoir thickness needed to store the fluids that have been produced at Larderello indicate thicknesses on the order of hundreds of meters to kilometers (see below). These conflicts can be reconciled by assuming that an individual well tends to tap a small number of features of high permeability (fracture zones?) which extend perhaps tens of meters and intersect other features; all of these ultimately connect to a much thicker section of interconnecting features of high permeability. The reservoir's effective thickness is great for the storage of fluids but small for the amount governing the resistance for flow to a well. Note that these zones of high permeability can be viewed as open fractures instead of a thin zone of brecciated rock. To have the same carrying capacity as 6.2 m of brecciated rock of 15.8 darcy permeability, an open fracture is only 0.226 cm thick (Muskat, 1946, p. 425). Sestini (1970, p. 635) states that in VC 10 "productive fissures were intercepted...at depths of 950 and 1030 m", but he does not elaborate on the term or how a productive fissure is recognized.

Plots for Gabbro 9 in the same coordinates as figure 11 (but not shown) look similar, but with different values. The permeability-thickness is 405 darcy-m. Using the Gewers and Nichols correlation, the permeability is 1050 darcy and the thickness 0.39 m. These are quite different numbers than for VC 10, but the wells are 7 km apart.

Relation of mass produced to decline in shut-in pressure

In the last section, the flow to a well from a reservoir at pressure P_o was analyzed. As large quantities of steam are withdrawn over a period of time, this reservoir pressure declines. The purpose of this section is to discuss the decline in reservoir (or shut-in) pressure and its relation to total mass withdrawn. The mass of fluids produced also bears on thickness of reservoir required and the percentage of liquid water in the undisturbed system.

The theory for relating mass produced to decline in shut-in pressure for a steam reservoir without liquid water and its application to The Geysers has been discussed by Ramey (1970a) and for two configurations of vapor-dominated reservoirs with liquid water by Brigham and Morrow (1974). Other configurations are possible (see e.g. White and others, 1971). The important point for our purposes is that the data for shut-in pressure P_o and total mass produced should be plotted as P_o/Z versus mass produced where Z is the gas law deviation factor at the current reservoir pressure and temperature. For a closed reservoir containing only steam and rock, the data would plot as a straight line. For other reservoirs, curvature and discontinuous slopes will appear. In their initial states, vapor-dominated reservoirs are strongly out of equilibrium with respect to hydrostatic pressures in surrounding rocks (White and others, 1971). Any recharge from surface waters must occur through zones of very high resistances; otherwise the reservoir should collapse and fill with liquid. Considering the high rates that such reservoirs can be produced compared to rates of discharge of initial surface seeps, a vapor-dominated reservoir is essentially a closed-volume system.

The data which we will consider is for the northeast zone of Larderello, including Larderello, Gabbri, and Castelnuovo (figure 1). The boundary shown in figure 1 is a somewhat extended version of the shut-in pressure contours presented by Ferrara and others (1970) for the years 1959 and 1969. There may be more than one reservoir within this boundary, but the data are too limited to detect this. Also, steam may be derived from a larger area than is shown. The curved southwest boundary is drawn along a pressure maximum. Even if the reservoir is continuous, mass to the southwest is flowing to other wells. The other boundaries are inferred to be closed because wells are scarce outside them; presumably wells were added continually until commercial quantities of steam were no longer found. Data for mass flow for this zone are given by Sestini (1970) for the period 1949 through 1969. (The outlined zone includes nearly every well in his subdivision 2.) The mass flow prior to 1949 has been obtained from power-production data (figure 27, ENEL, no date), using a steam consumption of 20 kg/kWh for turbines exhausting to the atmosphere (Chierici, 1964) and assuming all of the early power production was from the outlined zone. Figure 12 shows the two values of average P_o/Z versus mass produced, with corresponding dates at the top. The average pressure values were obtained by planimetering the pressure contours in Ferrara (1970) and the Z values for this pressure and a temperature of 241°C from Ramey (1970a). In 1959, the pressure at the north-eastern margin of the field where little mass had been produced was 35 ata (34.3 bars). Because of the distance of this margin from the center of the field, this pressure should reflect the initial pressure of the field, so P/Z value for this pressure is shown on the zero mass-

produced axis. That this point is significantly above the line is not surprising as this is usually the case in plotting gas reservoir data (Ramey, 1970a). There are obviously too few points to make any statement about whether or not the reservoir is following a straight-line depletion, but the extrapolation to zero pressure provides a useful estimate of the initial mass in place, which is 9 x 10" kg. If there is a steady-state production, as some investigators propose, data for later years would plot at some constant value of P/Z. The evidence from the three data points is that the reservoir is depleting, and does not yet have a steady state production value.

The quantity of mass initially in place of 9 x 10" kg, predicted from figure 12, could be less than the actual mass, but cannot be much too high because 5.3 x 10" had been produced by 1970. This initial mass may now be used to estimate how thick the reservoir might be and how much liquid water it contained in additon to vapor. Assuming a reservoir of horizontal area A, thickness L, porosity ϕ, and volume fraction of water in pores X at an initial uniform temperature, the stored mass is

$$M = \phi AL\left(\frac{X}{V_w} + \frac{(1-X)}{V_g}\right) \qquad (15)$$

where V_w and V_g are the specific volume of liquid and vapor, respectively. For the horizontal area, we use the boundary drawn in figure 1, so A = 56 km^2. We then use equation 15 to calculate the reservoir thickness L and water zone thickness L_w = XL as a function of ϕ and X. The calculation of a water-zone thickness L_w is a convenient number, but note that this liquid can reside both in a deep water-saturated body and

as finely dispersed pore water (White and others, 1971; Truesdell and White, 1975). Table 2 gives several sets of sample numbers, assuming that the steam and water are at 241°C. The top row of numbers assumes no liquid present (X = 0) and shows that the entire mass could have been stored as steam, but probably was not. A continuous reservoir of 0.05 porosity is unlikely to be maintained over 19 km of depth. A thickness of 5 km for 0.2 porosity might be more reasonable, but this is a very great depth to maintain this high a porosity. Allowing water to be present yields numbers which are quite a bit more reasonable. For example, a porosity of 0.1 with a water fraction of 0.1 of pore volume would store the required mass in a zone 1.7 km thick, and this is not an unreasonable thickness. The pervious zone at Larderello is normally considered to be Triassic evaporitic formation with impermeable formations above and below it (e.g. Cataldi and others, 1963). In the area of figure 1, the thickness of this formation varies from 0 to 300 m with an average thickness of 50 to 100 m. From the calculated thicknesses in table 1, this formation could store the required mass if it were filled with liquid water, but then Larderello would not be a vapor-dominated system but a hot-water system (White and others, 1971; Truesdell and White, 1975). Assuming the formations above and below the Triassic evaporites are porous but relatively impermeable, they could still contribute large quantities of steam by flow to the pervious formation and then to the wells because of the large surface areas involved.

The production of superheated steam from liquid water can take place in basically two ways (discussion based on Truesdell and White, 1975). Water could exist as a continuous liquid phase in a deep water

table. Lowering the pressure in the overlying steam zone would cause this water to boil. The temperature of the steam which boils off the deep water table can be above, below, or equal to the temperature in the steam zone depending on the initial temperature distribution of the deep water table and the salinity of the fluid (Truesdell and White, 1975). The second production mechanism is the boiling of pore water dispersed through the reservoir itself. If the fractional liquid saturation is below about 0.1 or 0.2, liquid will not flow in response to a pressure gradient but will boil in place. Because of the large amount of energy stored in the rock, boiling of a small volume-fraction of liquid water would change the reservoir temperature by only a few degrees to several tens of degrees (Celsius) (Truesdell and White, 1975). Pressures would continue to decrease in areas where all water had been boiled to steam. With these two production mechanisms it is not possible to settle on a value for average reservoir liquid fraction without more detailed data.

Conclusions

The calculations that have been presented are not adequate to describe all production patterns of the Larderello reservoir. The available published data are too scanty to build a systematic picture and the bottom-hole calculations have not been checked by field measurements. A major purpose in presenting these calculations is to show that bottom-hole temperatures rather than wellhead values must be considered to find significant variations. From the limited number of calculated bottom-hole temperatures and temperature-time patterns, different processes clearly are dominant in different parts of the reservoir. The outline of systematic variation must await the application of these techniques to a more detailed set of data.

The application of the theory for flow of steam to a well must be done with care. The relative constancy of calculated temperatures for two wells indicates that large quantities of liquid water cannot be boiling to steam in the near-well region. For some other wells, this is clearly not true, and the theory does not apply. The two wells analyzed seem to be fed by thin zones of rather high permeability, though this conclusion is based on using correlations for turbulence factor and permeability which may not actually apply. The conclusion that turbulence is important in these wells rests on the assumption that flow in the near-well region is simply the flow of steam. If the flow included a small amount of boiling near the well, the data plotted in figure 11 might look like non-Darcian flow. Until more detailed field data are obtained, the conclusion that turbulence effects are important is only tentative. Note that a technique which I have not applied is the

analysis of short-time well test data. The analysis of transient production and shut-in pressure data has become quite sophisticated in petroleum practice and is starting to be applied to geothermal fields (Ramey, 1970b), but has not yet been attempted in any detail at Larderello.

The limited data used to construct the plot of shut-in pressure decline versus mass produced for the northeast zone of Larderello prevent definitive conclusions concerning the path of reservoir depletion. If historical data are available, they should be analyzed by this technique to establish the depletion path.

ACKNOWLEDGEMENTS

I would like to thank A. H. Truesdell and D. E. White for the many stimulating discussions on vapor-dominated systems, H. J. Ramey, Jr. for comments on the manuscript and the Italian geothermal community for making so much of their data publicly available.

References cited

Boldizsár, T., 1963, Terrestrial heat flow in the natural steam field at Larderello: Geofisica Pura E Applicata--Milano, v. 56, p. 115-122.

Brigham, W. E. and Morrow, W. B., 1974, P/Z behavior for geothermal steam reservoirs: paper SPE 4899 presented at Soc. of Petroleum Engineers 44th annual Calif. Regional Meeting, San Francisco, April 4-5, 8 p.

Burgassi, R., Battini, F., and Mouton, J., 1964, Prospection géothermique pour la recherche des forces endogènes, in Geothermal Energy I: United Nations Conf. New Sources Energy, Rome, 1961, Proc., No.2, p. 134-140.

Cataldi, R., Stefani, G. and Tongiorgi, M., 1963, Geology of Larderello region (Tuscany): Contribution to the study of the geothermal basins: in Tongiorgi, E., ed., Nuclear Geology on Geothermal areas, p. 235-265.

Chierici, A., 1964, Planning of a geothermoelectric power plant: technical and economic principles, in Geothermal Energy II: United Nations Conf. New Sources Energy, Rome, 1961, Proc., v. 3, p. 299-311.

Elder, J. W., 1965, Physical processes in geothermal areas: in Lee, W. H. K., Ed., Terrestrial Heat Flow: A.G.U., p. 211-239.

_____, 1966, Heat and mass transfer in the earth--hydrothermal systems: New Zealand Dept. Sci. and Indus. Research Bull. 169, 115 p.

Ente Nazionale per L'Energia Elattrica,[No date], Larderello and Monte Amiata: Electric power by endogeneous steam.

Ferrara, G. C., Panichi, C. and Stefani, G., 1970, Remarks on the geothermal phenomenon in an intensively exploited field. Results of an experimental well: Geothermics Special Issue 2, v. 2, pt. 1, p. 578-586.

Gewers, C. W. W. and Nichol, L. R., 1969, Gas turbulence factor in a microvugular carbonate: Jour. of Canadian Petroleum Technology, v. 8, p. 51-56.

Katz, D. L., and Coats, K. H., 1968, Underground storage of fluids: Ann Arbor, Ulrich's Books, 575 p.

Katz, D. L., Cornel, D., Kobayashi, R., Poettmann, F. H., Vary, J. H., Elenbass, J. R., and Weinaug, C. F., 1959, Handbook of natural gas engineering: New York, McGraw Hill, 802 p.

Keenan, J. H., Keyes, F. G., Hill, P. G., and Moore, J. G., 1969, Steam tables. Thermodynamic properties of water including vapor, liquid, and solid phases: New York, John Wiley, 162 p.

Liepmann, H. W. and Roshko, A., 1957, Elements of gasdynamics: New York, John Wiley, 439 p.

Marchesini, E., Pistolesi, A. and Bolognini, M., 1962, Fracuture patterns of the natural steam area of Larderello, Italy, from airphotographs: Archives Internat. de Photogrammetrie, v. 14, Trans. of the Symposium on Photo Interpretration, Delft, p. 524-532.

Muskat, M., 1946, The Flow of Homogeneous Fluids Through Porous Media. J. W. Edwards, Ann Arbor, 763 pp.

Nencetti, Renzo, 1964, Méthodes et dispositifs de mesure en tête des puits employés au champ géothermique de Larderello après éruption d'un sondage, in Geothermal Energy I: United Nations Conf. New Sources Energy, Rome, 1961, Proc., v. 2, p. 326-338.

Pollastri, G., 1970, Design and construction of steam pipelines: Geothermics Special Issue 2, v. 2, pt. 1, p. 780-811.

Ramey, H. J., Jr., 1962, Wellbore heat transmission: Jour. Petroleum Technology, p. 427-435.

_____, 1970a, A reservoir engineering study of The Geysers geothermal field: Evidence Reich and Reich, petitioners v. commissioner of Internal Revenue, 1969 Tax Court of the United States, 52. T. C. No. 74, 1970.

_____, 1970b, Short-time well test data interpretation in the presence of skin effect and wellbore storage: Jour. Petroleum Technology, p. 97-104.

Rumi, O. 1967, Determination of the thermodynamic state of water vapor in steady adiabatic flow along a vertical pipe (wells): La Termotecnica, v. 21, no. 8, p. 407-414.

_____, 1970, Some observations about the thermo-fluid-dynamic behavior of the steam in the wells of Larderello and about the best exploitation conditions: Geothermics Special Issue 2, v. 2, pt. 1, p. 698-703.

_____, 1972, Some considerations on the flow-rate/pressure curve of the steam wells of Larderello: Geothermics, v. 1, no. 1, p. 13-23.

Sestini, G., 1970, Superheating of geothermal steam: Geothermics Special Issue 2, v. 2, pt. 1, p. 622-648 [1971].

Truesdell, A. H., and White, D. E., 1975, Production of superheated steam from vapor-dominated geothermal reservoirs: Geothermics (in press).

White, D. E., 1965, Geothermal energy: U.S. Geol. Survey Circ. 519, 17 p.

White, D. E., Muffler, L. J. P., and Truesdell, A. H., 1971, Vapor-dominated hydrothermal systems compared with hot-water systems: Econ. Geology, v. 66, p. 75-97.

Table 1.--Dimensions of wells discussed in text. Values in parentheses are estimated.

	Diameter (CM)	Total depth (m)	Depth to Steam Zone (m)	Thickness of Cover Rock,(m)
VC 10	32	1088	796	826
Gabbro 9	32		859	700
St. Silvestro	(32)		(700)	550
Prata 2	(32)		(700)	550
Prata 4	(32)		(700)	560
Larderello 85	(32)		(700)	400

Table 2.--Reservoir thickness L and water zone thickness L_w for different values of porosity ϕ and volume fraction of water X needed to store estimated initial mass in place for outlined zone of figure 1. Area = 56 km^2, mass = 9×10^{11} kg.

	ϕ	0.2	0.1	0.05
X = 0	L...m	4720	9440	18870
X = 0.01	L...m	3220	6430	12860
	L_w...m	32	64	129
X = 0.05	L...m	1420	2830	5660
	L_w...m	71	141	283
X = 0.10	L...m	832	1660	3330
	L_w...m	83	166	333
X = 0.20	L...m	456	913	1830
	L_w...m	91	183	365
X = 1.0	L...m	99	198	396

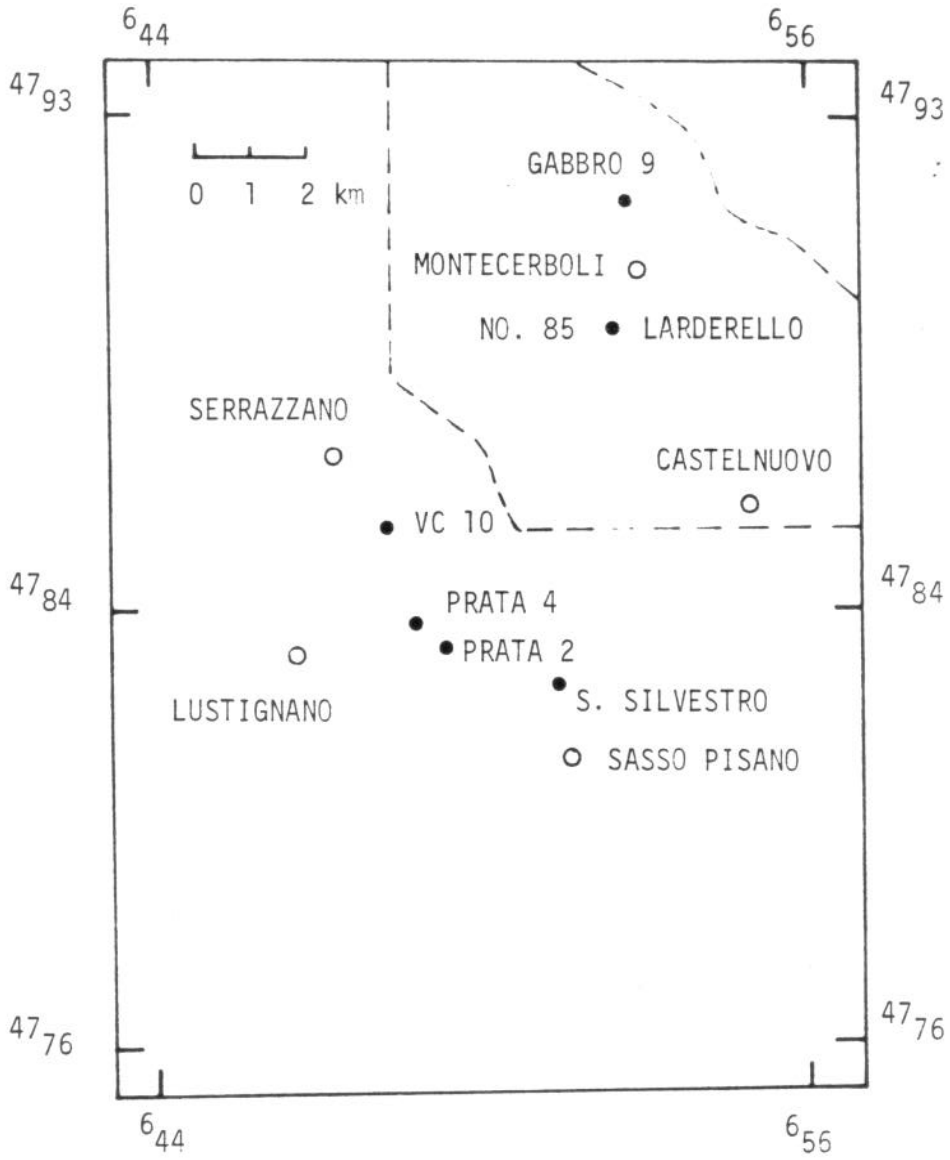

Figure 1.--Larderello geothermal area. Open circles are some of the towns. Closed circles are wells discussed in text. Broken line outlines northeast zone discussed in text.

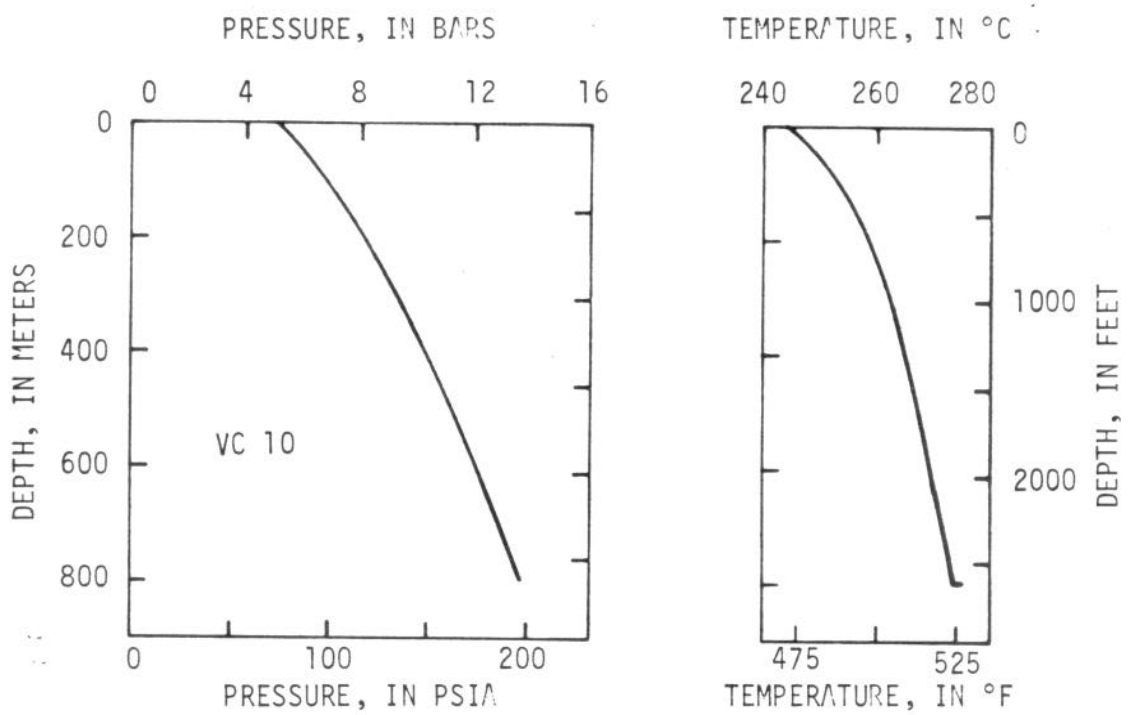

Figure 2.--Flowing pressures and temperatures in well VC 10 calculated from measured wellhead data. Mass flow = 37.5 kg/sec (298×10^3 lb/hr).

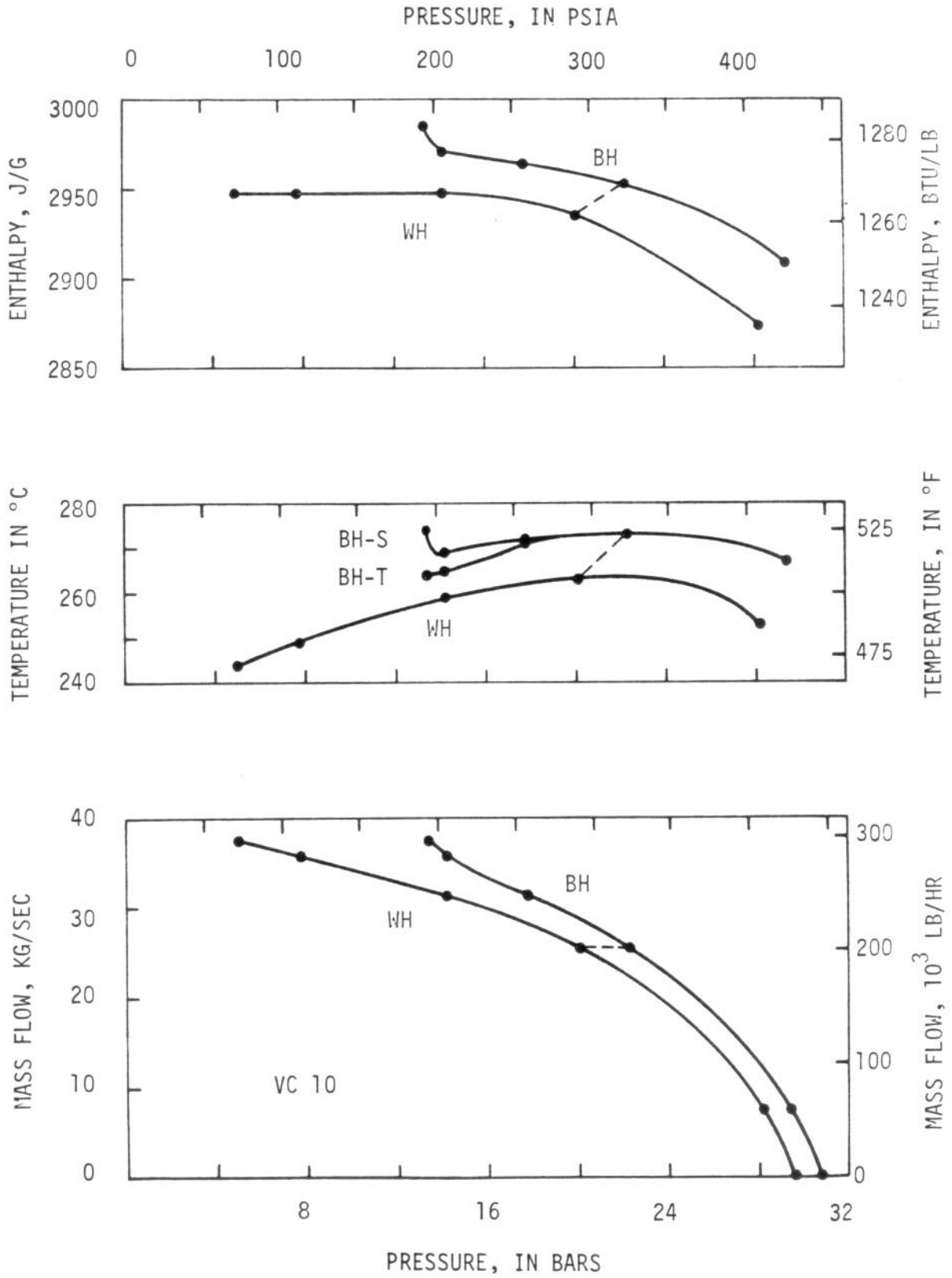

Figure 3.--Measured wellhead (WH) and calculated bottom-hole (BH) characteristics of well VC 10 in 1963. Calculated bottom-hole enthalpies assume that wellhead temperatures are static values. Calculated bottom-hole temperatures assume wellhead temperatures are static (BH-S) or total (BH-T) Corresponding points for one set of bottom-hole and wellhead conditions are joined by a broken line.

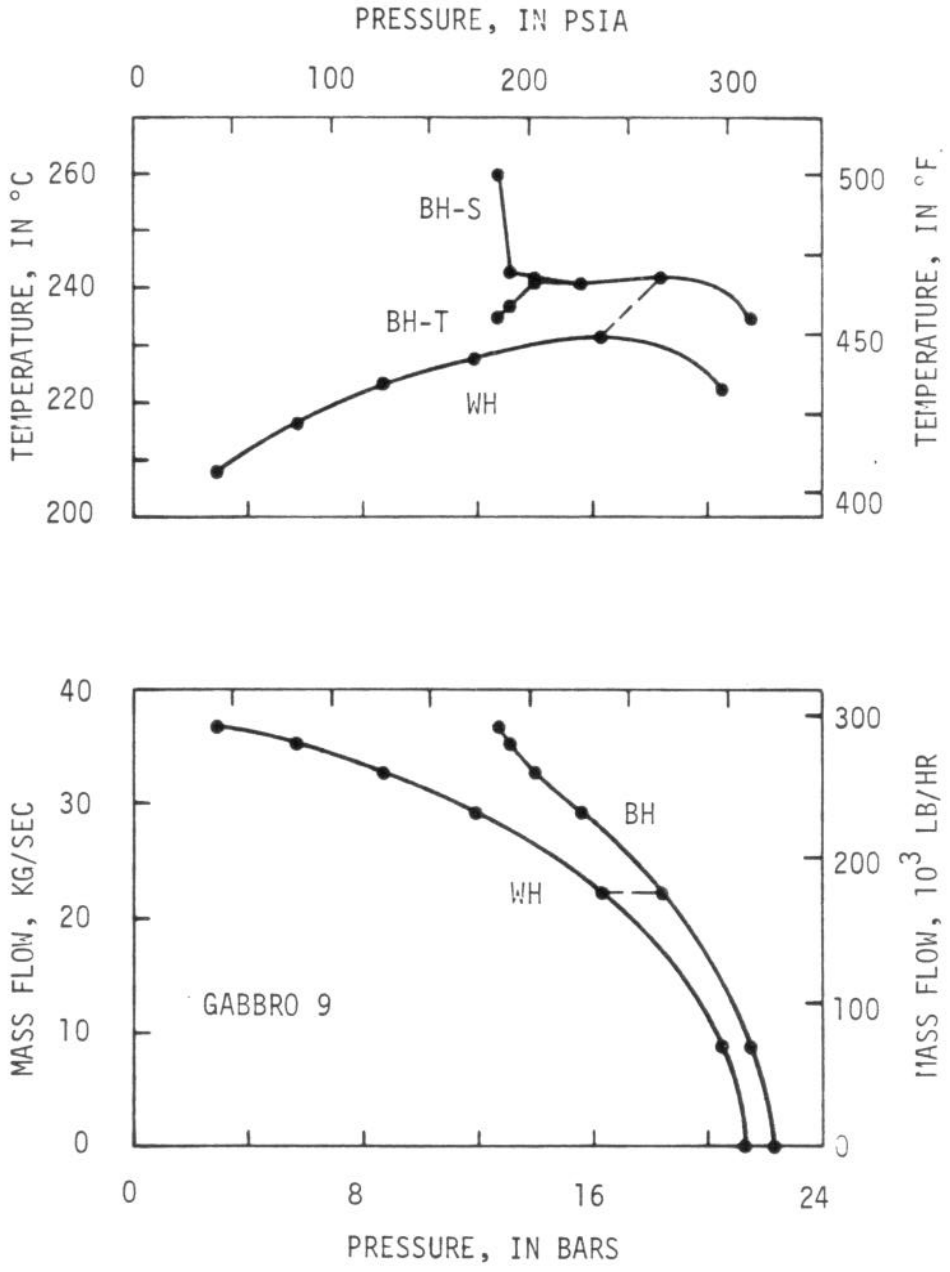

Figure 4.--Measured wellhead (WH) and calculated bottom-hole (BH) characteristics of well Gabbro 9 in 1966. Calculated bottom-hole temperatures assume wellhead temperatures are static (BH-S) or total (BH-T). Corresponding points for one set of bottom-hole and wellhead conditions are joined by a broken line.

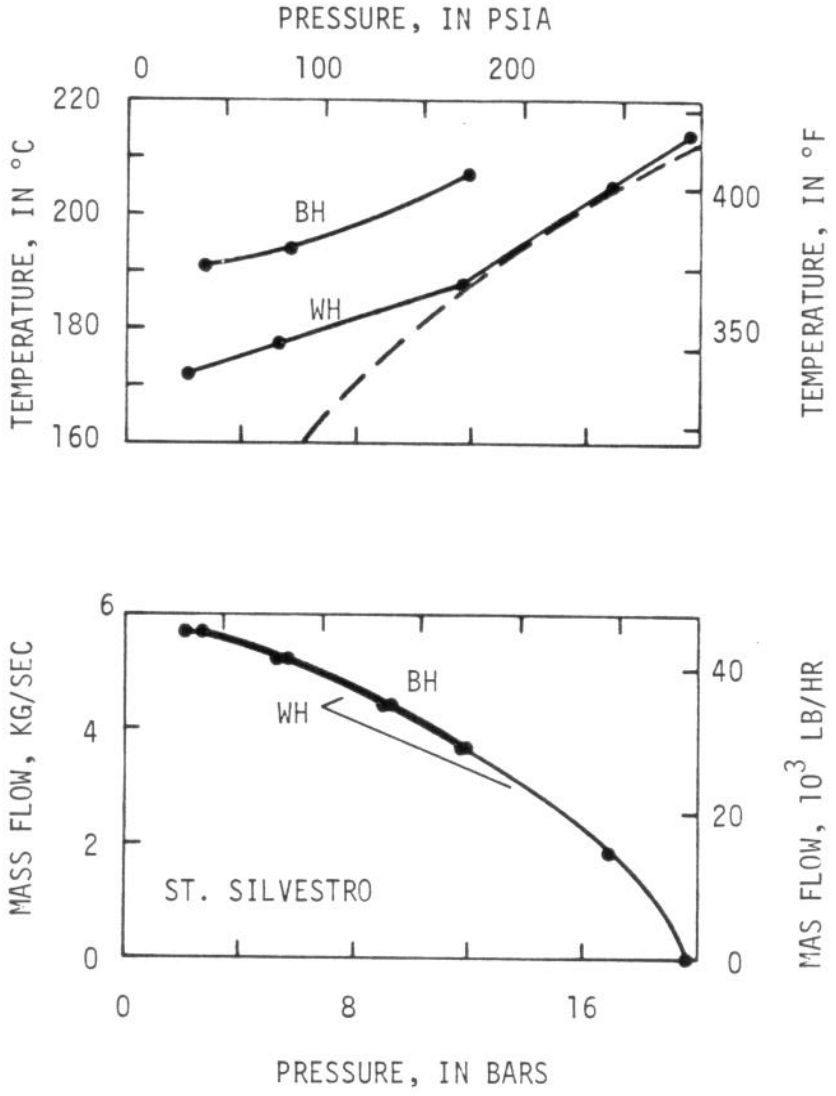

Figure 5.--Measured wellhead (WH) and calculated bottom-hole (BH) characteristics of St. Silvestro (Sasso Pisano). Broken line is saturation line for steam-water mixture.

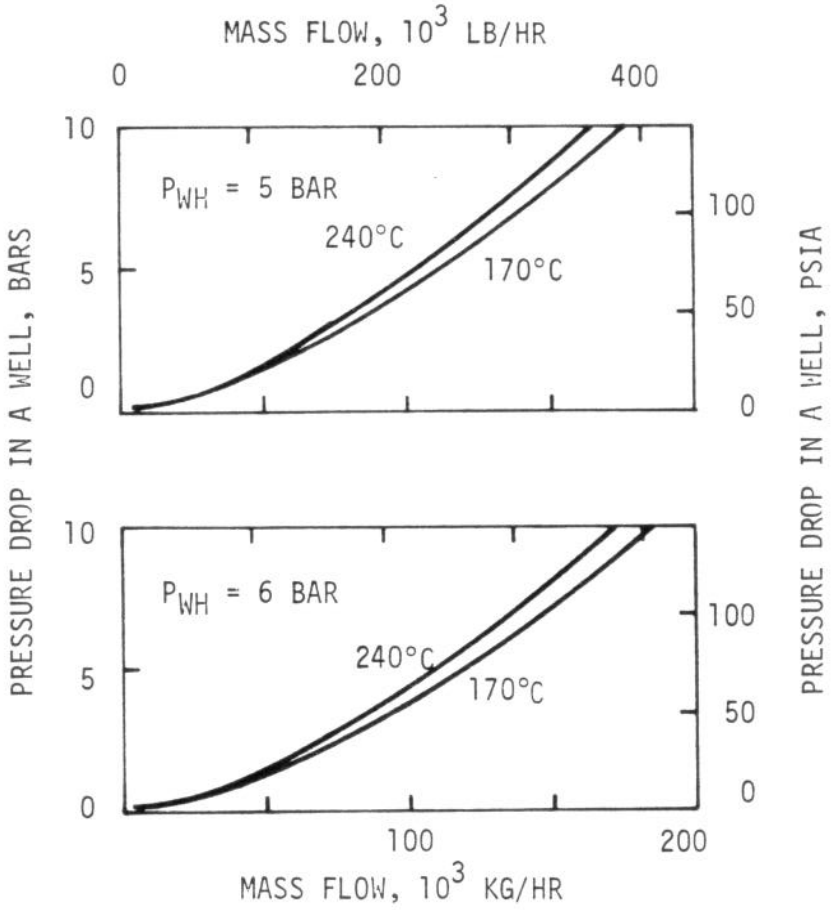

Figure 6.--Calculated pressure drops from bottom-hole to wellhead (p_{BH} - p_{WH}) for two wellhead pressures and two wellhead temperatures for a representative steam well.

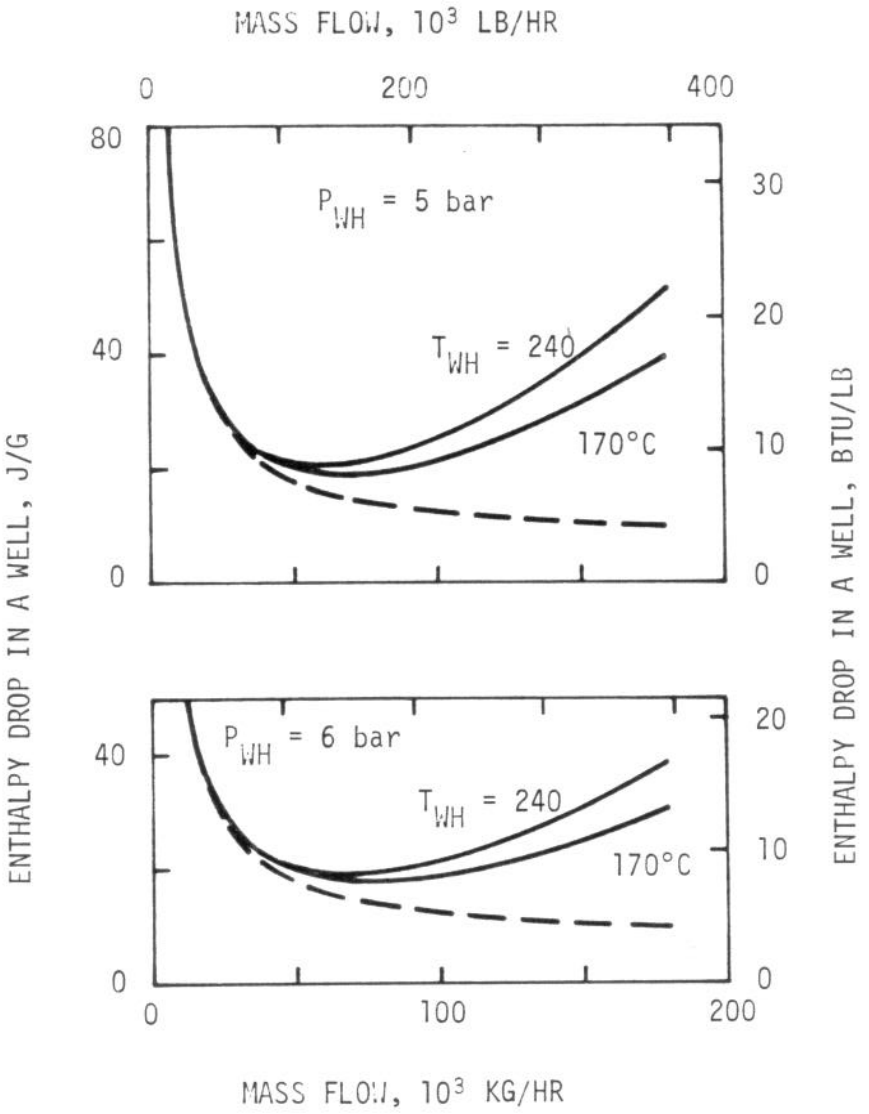

Figure 7.--Solid curves are calculated enthalpy drops from bottom-hole to wellhead ($h_{BH} - h_{WH}$) for two wellhead pressures and two wellhead temperatures assumed static for a representative steam well. Broken curves are change in total enthalpy. The differences between broken and solid-line curves are a measure of kinetic energy in flowing steam.

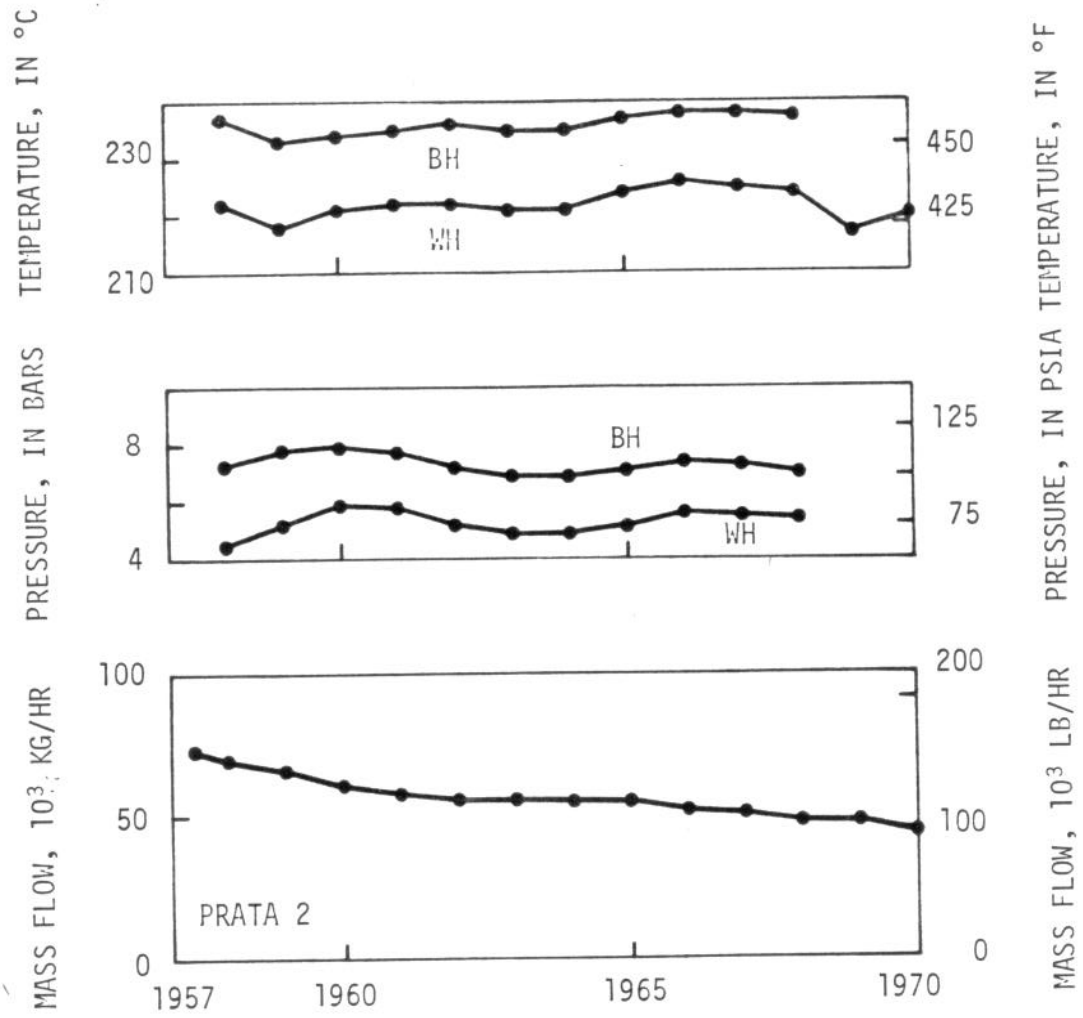

Figure 8.--Measured wellhead (WH) and calculated bottom-hole (BH) flow-time data for well Prata 2.

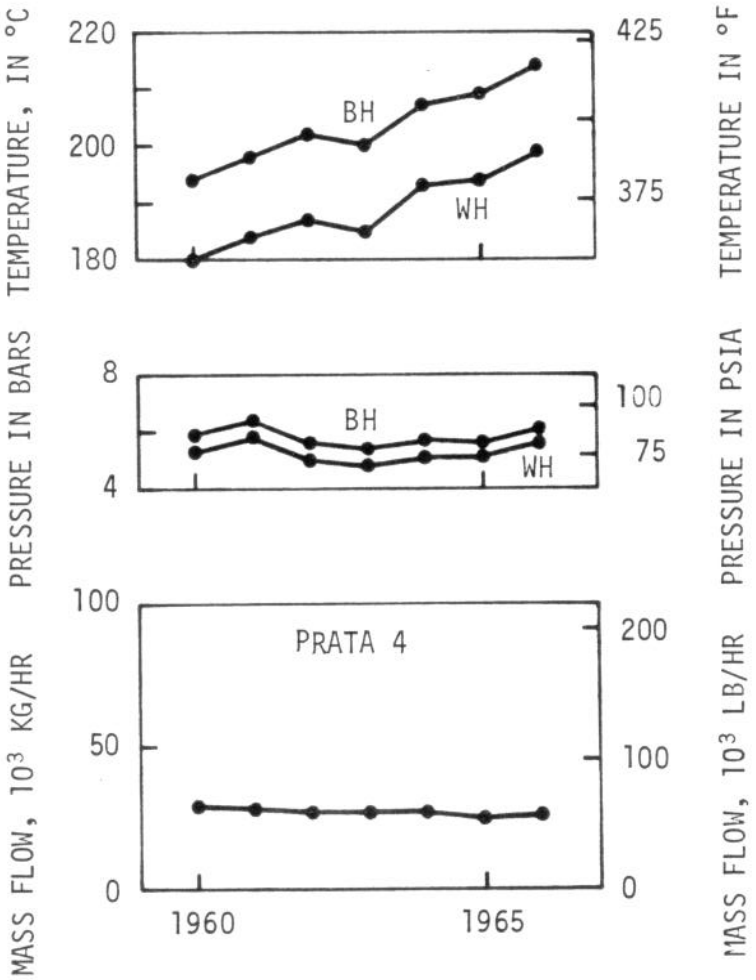

Figure 9.--Measured wellhead (WH) and calculated bottom-hole (BH) flow-time data for well Prata 4.

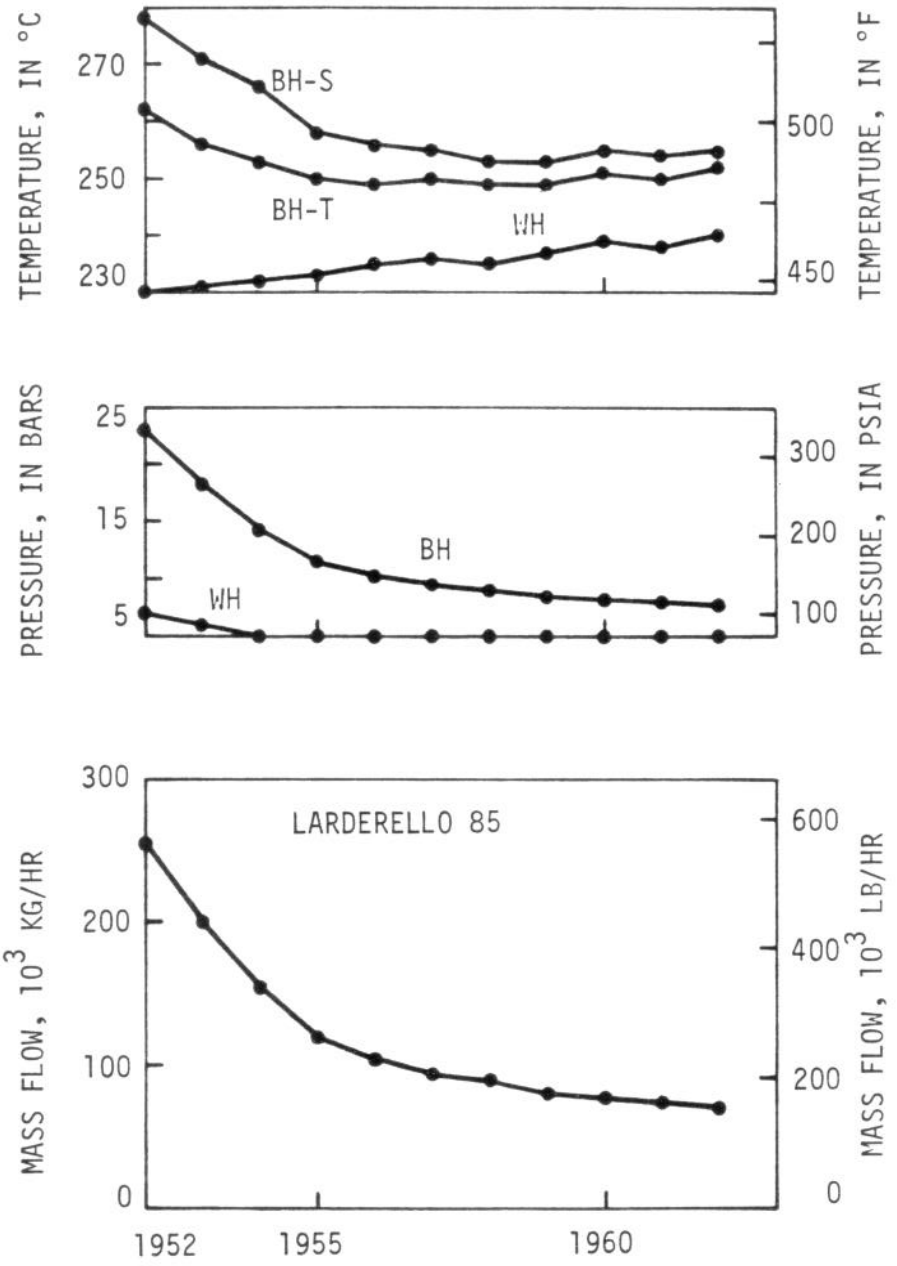

Figure 10.--Measured wellhead (WH) and calculated bottom-hole (BH) flow-time data for well Larderello 85. Bottom-hole temperatures calculated assuming wellhead temperatures are static (BH-S) or total (BH-T).

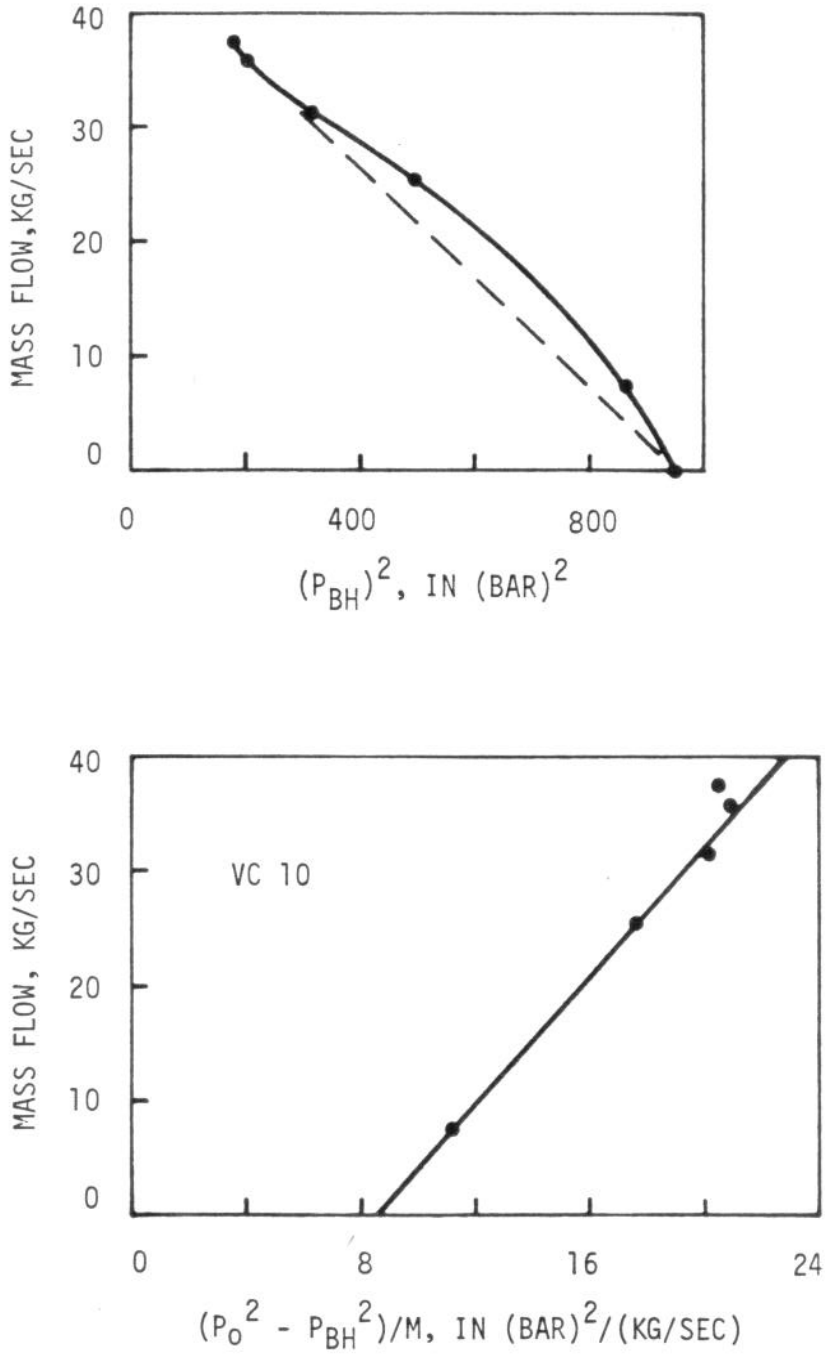

Figure 11.--Calculated bottom-hole data for VC 10 plotted to show the effect of turbulence term in equation 14.

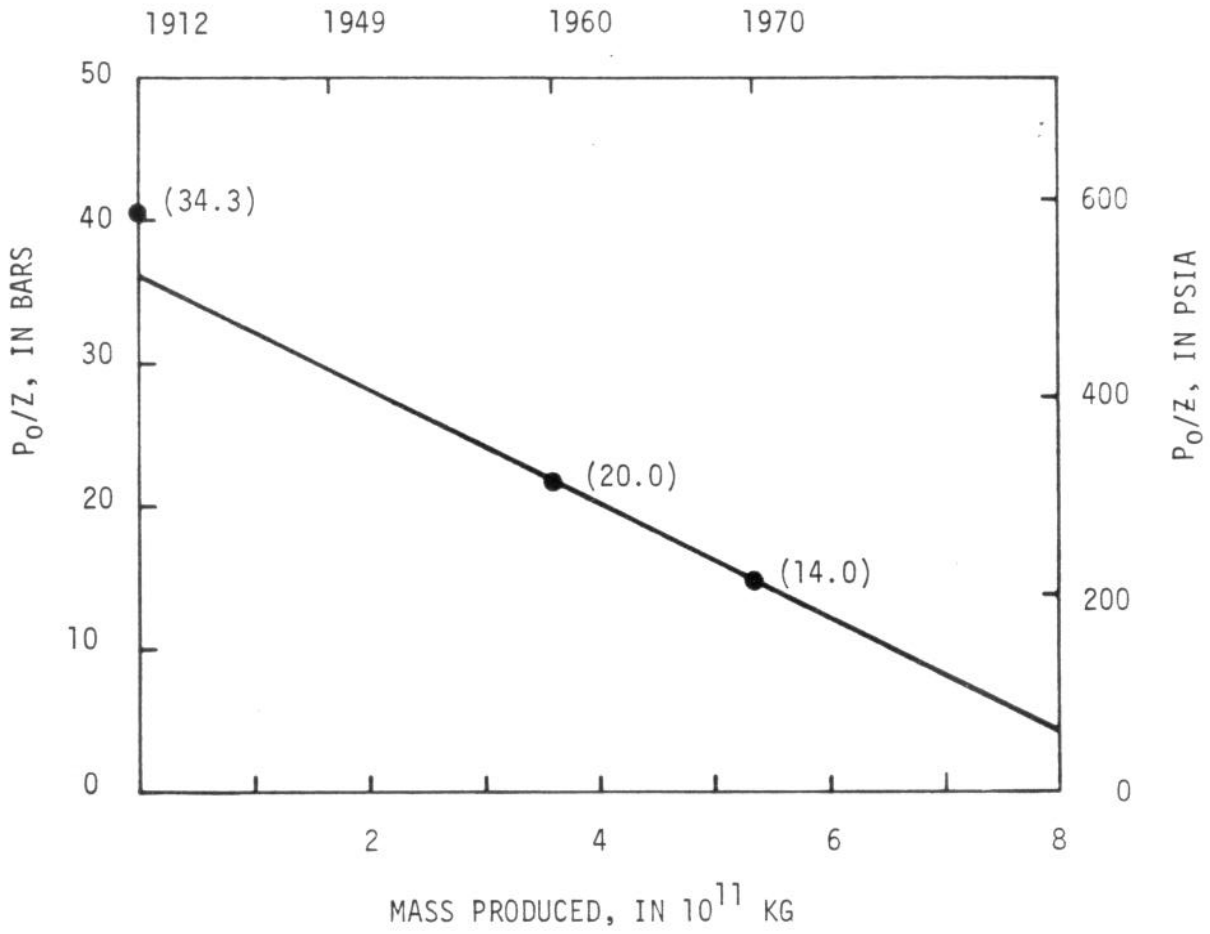

Figure 12.--Average reservoir pressure P_o divided by gas law deviation factor Z versus total mass produced for northeast zone of Lardrello as outlined in figure 1. Values in parentheses are average reservoir pressures.